Check for updates

Drag Reduction Performance of Mechanically Degraded Dilute Polyethylene Oxide Solutions

Yasaman Farsiani
Mechanical and Aerospace Engineering,
Oklahoma State University,
201 GAB,
Stillwater, OK 74078
e-mail: yasaman.farsiani@okstate.edu

Zeeshan Saeed
Mechanical and Aerospace Engineering,
Oklahoma State University,
201 GAB,
Stillwater, OK 74078
e-mail: zeeshan.saeed@okstate.edu

Brian R. Elbing[1]
Mem. ASME
Mechanical and Aerospace Engineering,
Oklahoma State University,
201 GAB,
Stillwater, OK 74078
e-mail: elbing@okstate.edu

Mechanical degradation of dilute solutions of polyethylene oxide (PEO) via chain scission was investigated within a turbulent pipe flow. Comparisons of the drag reduction performance with and without degradation were made by matching the onset of drag reduction conditions, which has been shown for PEO to be related to the mean molecular weight. The bulk flow behavior of both the degraded and nondegraded samples were generally consistent with trends observed in the literature, but a subset of conditions showed significant deviation in the slope increment (drag reduction performance) between the degraded and nondegraded samples. When they deviated, the degraded samples were consistently more efficient than the nondegraded samples even though they had the same mean molecular weight. The deviations were shown to scale with the normalized difference between the initial and final molecular weights. The current data and analysis as well as the literature suggest that the deviations in the polymer performance (slope increment) are related to changes in the molecular weight distribution. More specifically, the improved performance of the degraded samples relative to the nondegraded ones at the mean molecular weight of the degraded sample indicates an excess of longer polymer chains since the higher chain fractions in a degraded solution more effectively control the flow properties when within a certain degree of degradation and Reynolds number.
[DOI: 10.1115/1.4047118]

Keywords: polymer drag reduction, degradation, pipe flow, pressure drop, experimental

1 Introduction

The ability to reduce skin-friction with polymer solutions, historically referred to as Toms effect, has been known since the late 1940s [1–3]. Since that point, there have been numerous successful studies that have produced various applications [4] with most associated with internal flows [5,6]. Most active research in polymer drag reduction (PDR) focuses on developing a fundamental understanding of PDR to enable external flow applications such as marine vehicles [7–13], which in 2010 there was a successful application of PDR to improve ship speed on a sailing vessel [14]. One of the primary limiting factors for advancing PDR to external flows (as well as expanding internal flow applications) is polymer degradation. Polymer degradation is known to be dependent on many initiating factors such as oxidative and bacterial action, free radical interaction (chemical degradation), thermal degradation, and mechanical degradation [15–20]. The aging of polymer solution has also been found to contribute to polymer solution degradation [21]. This study, however, focuses solely on degradation due to chain scission induced from turbulent flow structure–polymer chain interaction (i.e., mechanical degradation in a turbulent pipe flow). Many theoretical/computational models detailing the mechanics of the physical process of polymer-chain degradation based on their interaction with the basic turbulent flow structures (e.g., horseshoe/hairpin vortices) are available [22–24].

While the literature for polymer degradation (mostly for internal flows) is vast, a brief review of key papers that influence this work is provided here for completeness. The flow-induced shear (mechanical force) on the polymer chain can be generated from abrupt changes in flow geometry (e.g., pumps, valves, and perforations [25]) or large mean velocity gradients such as those experienced at the wall of high Reynolds number turbulent flows [11,26–28]. Initial studies (e.g., Ref. [29]) discovered that it was extremely challenging to produce a setup that could isolate the degradation to the flow region of interest. Even more recent studies have frequently concluded that the majority of the degradation was produced at the entrance to their test facility [19,28,30].

Paterson and Abernathy [31] was one of the earliest investigations on the impact of flow-assisted (mechanical) degradation on the molecular weight distribution (e.g., polydispersity), which concluded that degradation influences the resulting flow properties. Yu et al. [32] used monodisperse polystyrene and polydisperse polyisobutene samples in oils under high shear rates to show that the molecular weight distribution narrowed for the polydispersed samples and only had a slight broadening of the monodispersed sample. More specifically, the distributions revealed that the breaking of the chains was not a random process. Hinch [33] developed a formula estimating the required force to break a molecular chain at a given location within the chain. This theoretical evaluation showed that the maximum strain developed in stretching the chain was at its center. Subsequently, Horn and Merrill [34] showed that turbulence-induced scission of macromolecules in dilute solutions preferentially breaks at the midpoint of the chain. Moreover, Odell et al. [35] studied extensional flows produced in cross slot devices with low molecular weight ($M_w < 10^6$) polyethylene oxide (PEO), which was at sufficiently low molecular weights for measurements of the molecular weight distribution. These results showed that the molecular weight distribution had another peak in addition to the original one at half the molecular weight, indicating scission of the chain at its midpoint. More recently, a simulation of flow-induced polymer chain scission [36] validated the midpoint scission hypothesis under the condition that the elongation rate was comparable to the critical elongation rate, and then the instantaneous segmental tensions

[1]Corresponding author.

Contributed by the Fluids Engineering Division of ASME for publication in the Journal of Fluids Engineering. Manuscript received July 17, 2019; final manuscript received April 18, 2020; published online May 25, 2020. Assoc. Editor: M'hamed Boutaous.

Downloaded from http://asmedigitalcollection.asme.org/fluidsengineering/article-pdf/142/9/091201/6537180/fe_142_09_091201.pdf by guest on 05 December 2021

 Copyright © 2020 by ASME

attains a maximum at the chain midpoint. This has the consequence of the resulting daughter chains having a rather narrow distribution. However, it was also demonstrated that when the elongational rate is much larger than the critical elongational rate, scission can occur in the partially coiled chains resulting in scission occurring farther from the midpoint. This likely has a significant impact within wall-bounded turbulent flows where the stress distribution varies significantly from the maximum at the wall to very weak away from the wall (e.g., pipe centerline or outside of a turbulent boundary layer).

Hunston and Zakin [37] used turbulent drag reduction (similar to this study), viscosity, and gel permeation chromatography (GPC) on polystyrene samples to assess the influence of concentration, molecular weight, and molecular weight distribution on flow-assisted (mechanical) degradation. This showed that the onset of drag reduction provided information about the largest molecules in the flow while the flowrate dependence was related to the shape of the top part of the molecular weight distribution. Gampert and Wagner [38] used laboratory synthesized straight molecular chain polyacrylamide (PAM) in aqueous solutions to investigate the influence of molecular weight and polydispersity on drag-reducing effectiveness. Gampert and Wagner [38] artificially created polydispersity by mixing the high and low synthesized molecular weights in a single solution. This work made several conclusions that are consistent with available literature. Primarily, that the long-chain molecules are pivotal in determining the flow properties of a solution due to their preferential mode of extension and hence degradation, when the difference in size of existing chains in a solution is reasonably high within a suitable Reynolds number range.

Historically, mechanical degradation has significantly limited the viable applications for PDR since polymers are generally more efficient at reducing drag (i.e., require lower concentrations to achieve a desired drag reduction) the longer the polymer chain (i.e., higher molecular weight), but the longer the polymer chain the more susceptible it is to chain scission. Internal flows have typically avoided this problem by using stiffer polymers (e.g., PAM), and some applications have shown an increase in resistance to mechanical degradation with increasing concentration [39]. But the use of commercial grade PAM is not suitable for investigations involving the influence of molecular weight on drag reduction and mechanical degradation because they have a branched chain formation and the presence of copolymers [38]. Instead, PDR studies have focused primarily on high molecular weight PEO, as has been the case in external flow studies, because PEO has the ability to achieve maximum drag reduction (MDR) with relatively low concentrations ($\sim$10 parts-per-million (ppm)) when the molecular weight is sufficiently high [40]. In addition, PEO avoids the rheological issues faced with commercial grade PAM. The high efficiency of PEO is ideal for external flows, which continuously dilute the injected polymer solution into the developing boundary layer. However, as a result, polymer degradation has had a significant impact on PDR external applications and even the ability to study PDR within turbulent boundary layers.

Elbing et al. [11] developed a fundamental scaling law for the evolution of the mean molecular weight within a developing high-shear turbulent boundary layer, which requires an estimate of the steady-state molecular weight for the given local shear rate. This was produced from the universal scaling law for chain scission [41], given that the nominal bond strengths for carbon-carbon and carbon-oxygen bonds are 4.1 nN and 4.3 nN [42], respectively. In light of this observation, a review of literature that has reported PDR modifications to the near-wall velocity profile of a turbulent boundary layer with PEO [12,26,27,43–45] shows that many of the reported conditions [12,26,27] experienced significant changes in the mean molecular weight between the injection and measurement locations even though this was not accounted for in their analysis. This is particularly problematic when studying high drag reduction (HDR; >40% drag reduction), which recent

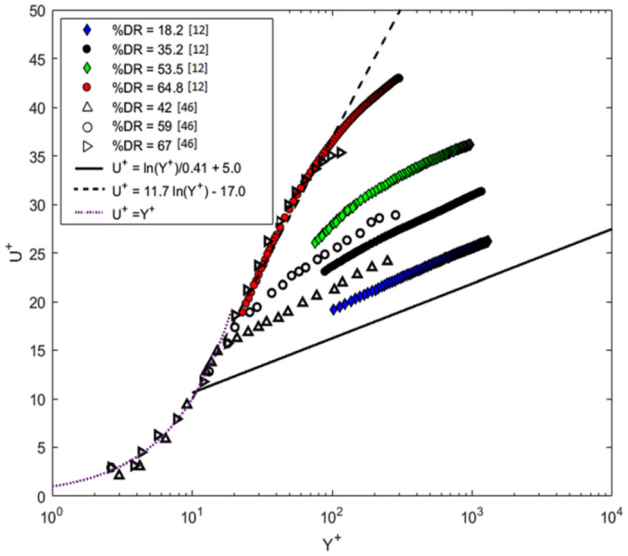

Fig. 1 Polymeric velocity profiles from a turbulent boundary layer with nonuniform concentration distribution [12] and channel flow with a constant concentration [46], which shows an increasing slope with increasing drag reduction for HDR (DR > 40%)

computational [46] and experimental [12,47] work (see Fig. 1; where the streamwise velocity and wall-normal distance are scaled with inner variables) has shown that modifications to the near-wall velocity profile deviate from the classical view that assumes the near-wall momentum distribution is independent of polymer properties. Elbing et al. [12] showed that Reynolds number was insufficient to collapse the available experimental turbulent boundary layer data, which suggests that the remaining scatter in the results must be related to polymer properties. These polymer properties are sensitive to the molecular weight, which means that in addition to an evolving polymer concentration distribution, there is also an evolving molecular weight distribution that needs to be accounted for to properly study HDR in a turbulent boundary layer. Recently, this has motivated an alternative approach, which is to develop a polymer ocean at a uniform concentration that has been mechanically degraded to a steady-state molecular weight [48,49]. Then the developing boundary layer would have a known and uniform polymer concentration and molecular weight. However, this requires a proper understanding of the impact of mechanical degradation via chain scission on the drag reduction performance of PEO, which is the focus of this study. Specifically, this study prepares degraded and nondegraded samples at the same mean molecular weight and does a comparative analysis of their drag reduction performance.

2 Experimental Method

2.1 Polymer Preparation. Polyethylene oxide was the only polymer used in this study, which has a structural unit (monomer) of $(-O-CH_2-CH_2-)$ that results in a polymer backbone consisting of carbon–carbon (C − C) and carbon–oxygen (C − O) bonds. Five molecular weights of PEO were tested with manufacturer specified mean molecular weights of 0.6, 1.0, 2.0, and 5.0×10^6 g/mol (Sigma Aldrich) and 4.0×10^6 g/mol (WSR301, Dow chemical). As previously stated, these high molecular weight polymers are highly susceptible to mechanical degradation within shear flows. Degradation depends on the molecular weight, polymer concentration, solvent type, turbulent intensity, and flow geometry [50,51].

Stock batches of relatively high concentration (1000–5000 ppm) polymer solution were prepared while filling a

Downloaded from http://asmedigitalcollection.asme.org/fluidsengineering/article-pdf/142/9/091201/6537180/fe_142_09_091201.pdf by guest on 05 December 2021

Table 1 Summary of the range of molecular weights and concentrations tested in this study as well as the corresponding intrinsic viscosity and overlap concentration for the given molecular weight PEO

$M_w \times 10^{-6}$ (g/mol)	C range (ppm)	$[\eta]_0$ (cm^3/g)	C^* (ppm)
0.6	100–500	402	2500
1	500	598	1680
2	50–500	1030	975
4	5–100	1760	568
5	5–20	2100	477

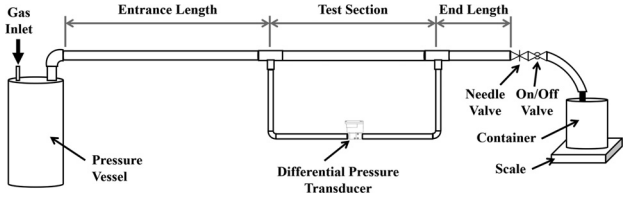

Fig. 2 Schematic of the pressure drop apparatus used for characterization of the polymer samples as well as mechanically degrading samples

larger reservoir with water. The dry powder was sprinkled into the jet of water filling the reservoir prior to contacting the free surface to avoid formation of polymer aggregates. These stock polymer solutions were then allowed to hydrate until solutions were homogeneous (8–24 h), with the longer hydration time required for higher molecular weight samples. Chlorine in the solvent (water) is known to cause polymer degradation [52,53], which the chlorine levels in the water supply for this study showed degradation after 12 h of exposure. Consequently, solutions that required hydration times longer than 12 h had the background chlorine removed by adding trace amount of sodium thiosulfate, which residual sodium thiosulfate and the resultant products of the reaction with chlorine has been shown to not impact the PDR performance [53]. Note that it was confirmed that the period of time required for the sodium thiosulfate to react with the chlorine was less than 12 h. Once fully hydrated, the stock solutions were diluted to the desired test concentration a few minutes prior to testing in the pressure vessel used to deliver the sample to the pressure drop apparatus.

Polymer solution concentrations are broadly categorized as dilute, semidilute, and concentrated. In the dilute regime, each polymer chain is sufficiently distant from other polymer chains such that there is minimal interaction between chains. As the concentration increases, polymer chains eventually begin to overlap and become entangled, which these interactions alter the polymer properties. As the concentration further increases from semidilute to the concentrated regime, molecules cannot move freely and significant interpenetration occurs due to the lack of space. These changes are identified from their rheological properties [54]. The critical overlap concentrations C^* and C^{**} define the transition points from dilute to semidilute and semidilute to concentrated regimes, respectively. The first overlap concentration can be found from the inverse of the intrinsic viscosity $([\eta]_0)$, $C^* = [\eta]_0^{-1}$, which $[\eta]_0$ can be estimated from the Mark-Houwink relationship [55], $[\eta]_0 = 0.01248\, M_w^{0.78}$. Table 1 provides the range of molecular weights and concentrations tested for degraded and nondegraded samples in this study as well as the corresponding intrinsic viscosity and C^*. The first overlap concentration was well above the test range at each molecular weight and, consequently, all testing was with dilute solutions.

A comparison between Table 1 and all of the subsequent nondegraded and degraded results shows that there are several conditions that were tested that are not discussed in this paper. This was required because the exact amount of degradation could not be known a priori due to the sensitivity of the exact flow configuration and flowrate. Consequently, a wide range of additional conditions had to be tested so that by trial-and-error a subset of conditions could be identified that produced degraded samples that matched molecular weights of available nondegraded samples. When the degraded molecular weight was within 10% of an available nondegraded sample, it was considered a viable test condition. That condition would then be repeatedly tested to confirm that it was repeatable and that the preparation procedures could reliably reproduce it.

2.2 Test Facility and Instrumentation. The primary test facility was a pressure drop apparatus that was used to characterize polymer properties and acquire the gross flow behavior. A schematic of the setup is shown in Fig. 2, including the pipe as well as the instrumentation. Test samples were placed in an 18.9-L 316 L stainless steel pressure vessel (740560, Advantc, Dublin, CA), which was sealed and pressurized to ~275 kPa during testing. A dip tube drew the polymer sample from the bottom of the pressure vessel and then pushed it into the pipe flow portion. It consisted of a 10.9 mm inner diameter (d) instrument grade seamless 316 stainless steel pipe (SS-T8-S-035-20, Swagelok) that was divided into three sections; the entrance length that was 150 d long to achieve fully developed turbulent pipe flow, a 1.05 m long test section and the end (exit) length that had a V-shaped, 4.8 mm orifice needle valve at the outlet to control flowrate (this valve was also used as the primary means to accelerate the degradation of the polymer solutions). Given the valve properties and the current operation range, the maximum flow coefficient was nominally 0.22. The pressure drop across the test section was acquired at various Reynolds numbers with a differential pressure transducer (PX2300-5DI, Omega Engineering). The mass flowrate, and ultimately the average velocity within the pipe, was determined by measuring the fill time with a stopwatch (RS-013, Pro-Coach) and the associated mass of the sample on a 35 kg digital balance (CPWplus-35, Adam Equipment). A more detailed discussion of the setup, instrumentation, and uncertainty quantification is provided in Lander [56]. A summary of the uncertainty analysis is provided below for completeness.

Polymer solution temperature was measured with a thermometer (25–125 °F, TEL-TRU, Rochester, NY) and was held relatively constant throughout testing at 21 ± 0.4 °C with a corresponding mean density (ρ) and kinematic viscosity (ν) of 998 kg/m^3 and 1.0×10^{-6} m^2/s, respectively. The pipe diameter and pressure drop length had uncertainties below 1%. Given the high accuracy of the pressure transducer (±0.25%), the largest uncertainty in the differential pressure was due to the experimental setup. Specifically, the holes (pressure taps) in the pipe walls required for the measurements were the largest source of error. Corrections were applied following the approach outlined in McKeon [57] with the corresponding uncertainty of ~3% for the pressure measurement. There are several sources of uncertainty that were considered for the mass flowrate measurement [56], but the largest source was the limitation of human reaction times. This resulted in uncertainties as large as 3%, but by increasing the measurement period (especially for low flowrate conditions), this uncertainty was reduced.

Propagating all sources of uncertainty results in uncertainties that significantly vary with flow condition, which the Prandtl–von Kármán (P–K) coordinates $\mathrm{Re}\sqrt{f}$ and $1/\sqrt{f}$ had typical uncertainties of ~6%. However, at low flowrates (i.e., at and below the onset of drag reduction) the uncertainty increases rapidly to well above 10% [56]. For these reasons, measurements at the onset of drag reduction were not attempted, but rather measurements at higher flowrates with uncertainty below 10% were curve fitted and then extrapolated back to the onset condition. Subsequently, the analysis focuses on the variations of the curve fit slopes, so a more detailed uncertainty analysis on the impact of these

Downloaded from http://asmedigitalcollection.asme.org/fluidsengineering/article-pdf/142/9/091201/6537180/fe_142_09_091201.pdf by guest on 05 December 2021

uncertainties in the P–K coordinates on the slope and intercept of the curve fits was performed. Here, error was introduced to each of the P–K coordinates such that a logarithmic curve fit takes the form of $1/(\sqrt{f}+\epsilon_o) = C_o \ln(\mathrm{Re}\sqrt{f}+\epsilon_1) + C_1$, where C_o, C_1 are constants and ϵ_o, ϵ_1 are the uncertainties in f and $\mathrm{Re}\sqrt{f}$, respectively. Some algebraic manipulation and expanding the resulting expression in a binomial form results in

$$\frac{1}{\sqrt{f}}\left(1-\frac{\epsilon_o}{2f}+\cdots\right) = C_o \ln\left(\mathrm{Re}\sqrt{f}\right) + C_o \ln\left(1+\frac{\epsilon_1}{Re\sqrt{f}}\right) + C_1$$

Neglecting higher order terms and some addition rearranging reduces the relationship to

$$\frac{1}{\sqrt{f}} = C_o \ln\left(\mathrm{Re}\sqrt{f}\right) + C_o \ln\left(1+\frac{\epsilon_1}{\mathrm{Re}\sqrt{f}}\right) + C_1 + \frac{\epsilon_o}{2f^{1.5}}$$

Treating the error sources as being nominally constants, this shows that the uncertainty impacts the intercept more than the slope when $\mathrm{Re}\sqrt{f}$ is large (current data $\mathrm{Re}\sqrt{f} \sim 10^3$).

Like many previous degradation studies [19,28,37,50,58], this work utilizes the drag reduction performance (determined from its behavior in this pressure drop apparatus) to investigate degradation. GPC and other such methods are preferred since they provide direct measurements of the molecular weight distribution, but GPC has proven to be impractical for high molecular weight PEO due to significant uncertainties in the analysis. One of the main issues that complicate this approach is that while PEO is soluble in tetrahydrofuran, a common eluent for GPC, it is isorefractive with tetrahydrofuran. This makes it so that it cannot be seen in that solvent with either index of refraction or light scattering detectors [14]. Another significant limitation in the use of GPC for estimating the polydispersity comes from its incapability to resolve low molecular weight fractions for PEO molecular weights as low as 2.5×10^5 g/mol [59]. Such lower molecular weight fractions are known to significantly affect the number average molecular weight of a sample necessary to evaluate polydispersity [38,59]. This renders the use of GPC for high molecular weight samples ineffective and so has not been made use of in this investigation. Thus, this study quantifies the impact of mechanical degradation via chain scission on the drag reduction performance of PEO primarily from the resulting variations in the turbulent drag reduction performance. Based on previous studies using other polymer solutions, the likely impact on the molecular weight distribution is inferred.

3 Results

3.1 Nondegraded Bulk Flow Characterization. It is common to present pipe flow skin-friction results in either a Moody diagram (Darcy–Weisbach friction factor versus Reynolds number) or in P–K coordinates ($f^{-1/2}$ versus $\mathrm{Re}_d f^{1/2}$). P–K coordinates are used for this study, where Re_d $(= \rho V d/\mu)$ is pipe diameter-based Reynolds number, f is the Fanning friction factor $(f = 2\tau/\rho V^2)$, ρ is the fluid density, V is the mean velocity, d is the pipe diameter, μ is the fluid dynamic viscosity, and τ is the wall shear stress. Assuming fully developed pipe flow, the wall shear stress (τ) is directly related to the pressure drop across a given length of pipe $(\tau = \Delta p\, d/4\,\Delta x)$, where Δp is the pressure drop measured over the pipe length Δx. The physical significance of P–K plots is that the ordinate is the ratio of the bulk fluid velocity to the turbulent friction velocity (divided by $\sqrt{2}$) and the abscissa is the ratio of the pipe diameter (outer length scale) to the viscous wall unit (inner length scale) (multiplied by $\sqrt{2}$). The skin-friction curve for Newtonian turbulent pipe flow in these coordinates is well represented by the P–K law, Eq. (1). Newtonian (water) results from the current setup are included in Fig. 3. These results are well approximated by the P–K law, which is also included for comparison.

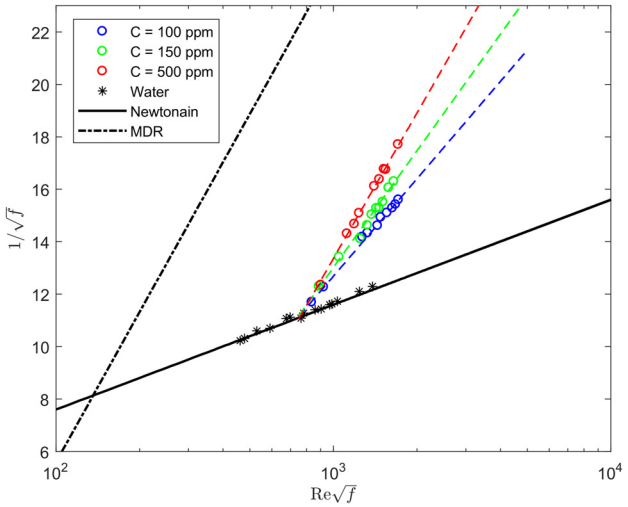

Fig. 3 P–K plot of 2×10^6 g/mol PEO at concentrations of 100, 150, and 500 ppm, as well as water (Newtonian) data at the same range of $\mathrm{Re}\sqrt{f}$. Included for reference are the P–K law, MDR asymptote, and logarithmic best-fit curves to the data within the polymeric regime.

$$\frac{1}{\sqrt{f}} = 4.0 \log_{10}\left(\mathrm{Re}_d\sqrt{f}\right) - 0.4 \tag{1}$$

With the addition of drag reducing polymer (PEO) solution, the results are shifted above the P–K law. The amount of increase is limited by the empirically derived MDR asymptote [60] given in Eq. (2). This study focuses on results within the polymeric region, which is at intermediate drag reduction levels between the MDR asymptote and the P–K law. The data within the polymeric regime are fitted following the form given in Eq. (3) [61]. Here, δ is the slope increment and W^* is the onset wave number, which both are dependent on the polymer properties. Furthermore, the slope increment (δ) is the change in slope relative to the P–K law slope, and the onset wave number (W^*) can be shown to be equal to the reciprocal of the viscous wall unit at the onset of drag reduction. The onset of drag reduction is identified by the intersection of the P–K law and the polymeric data fitted with Eq. (3). Note that below this minimum shear rate required to initiate drag reduction, the polymer solutions follow the P–K law, which is indicative of the need for a sufficient amount of shear to stretch the polymer chains and activate the drag reduction mechanism [62,63]. The onset of drag reduction for a given polymer type and molecular weight has been shown to have a negligible dependence on the concentration [30,61]. Current polymeric results using PEO at a $M_w = 2 \times 10^6$ g/mol and at concentrations from 100 to 500 ppm are also provided in Fig. 3. These results show that the slope increment increases with increasing polymer concentration (C) while the onset of drag reduction (intersection of P–K law and polymeric data fit) remains nearly constant for all three samples tested.

$$\frac{1}{\sqrt{f}} = 19.0 \log_{10}\left(\mathrm{Re}_d\sqrt{f}\right) - 32.4 \tag{2}$$

$$\frac{1}{\sqrt{f}} = (4.0+\delta)\log_{10}\left(\mathrm{Re}_d\sqrt{f}\right) - 0.4 - \delta\log_{10}\left(\sqrt{2}dW^*\right) \tag{3}$$

While the onset of drag reduction remains constant for a given molecular weight, it is sensitive to the mean molecular weight. Generally, the higher the M_w the lower the Reynolds number at the onset of drag reduction. Vanapalli et al. [30] compiled PEO data [61] to establish an empirical relationship between the onset of drag reduction shear rate (γ^*) and the mean molecular weight

Downloaded from http://asmedigitalcollection.asme.org/fluidsengineering/article-pdf/142/9/091201/6537180/fe_142_09_091201.pdf by guest on 05 December 2021

Table 2 Summary of nondegraded samples tested in the pressure drop apparatus as well as the resulting slope increment (δ), onset wave number (W^*), and the shear rate at the onset of drag reduction (γ^*)

$M_w \times 10^{-6}$ (g/mol)					
Manufacturer	Calculated	C range (ppm)	δ	W^* at $C_{\max}$ (m^{-1})	γ^* (s^{-1})
0.6	0.55	100–500	3.1–7.5	85,200	6090
1	1.1	500	13.5	71,900	3050
2	1.7	50–500	5.2–14.5	47,700	1950
4	3.7	5	6.13	30,900	900
5	4.8	5	7.5	27,800	697

The manufacturer specified molecular weight is provided as well as that determined from the onset of drag reduction [30].

(M_w), $\gamma^* = 3.35 \times 10^9/M_w$. This allows for the mean molecular weight to be determined if the wall shear rate at the onset of drag reduction is known. The wall shear rate at the onset of drag reduction is determined by calculating the intersection between the polymeric best-fit curve and the P–K law. The intersection provides the corresponding onset of drag reduction Fanning friction factor (f^*) and the onset of drag reduction Reynolds number (Re_d^*). Given the definition of the Fanning friction factor and the relationship between shear stress and shear rate at the wall ($\gamma = \tau/\rho\nu$), the onset shear rate at the onset of drag reduction can be determined from f^*, $\gamma^* = V^2 f^*/2\nu$. Thus, the mean molecular weight of the PEO polymer solutions can be inferred from the P–K plots. Table 2 provides a summary of the nondegraded conditions tested, including mean molecular weight (M_w) (both the manufacturer specified and that determined from the onset of drag reduction [30]), the resulting slope increment (δ), onset wave number (W^*), and the shear rate at the onset of drag reduction (γ^*). Note that most of the calculated mean molecular weights are slightly below the manufacturer specifications, which is consistent with past observations. These results demonstrate that the onset of drag reduction does vary with mean molecular weight since the molecular weights shown are consistent with the manufacturer specified values.

3.2 Degraded Bulk Flow Characterization. It is well documented that when the wall shear rate is sufficiently large, mechanical degradation via chain scission is possible [11,32,37]. While a universal scaling law for chain scission based on the molecular bond strength [41] is available, PEO has an established empirical relationship for the shear rate at the onset of degradation (γ_D) for a given mean molecular weight, $\gamma_D = 3.23 \times 10^{18} M_w^{-2.20}$ [30,64]. If the shear rate exceeds γ_D, the polymer chains will break and the mean molecular weight will decrease. Within the polymeric regime on a P–K plot, this is realized as data deviating from the logarithmic curve at higher $\mathrm{Re}\sqrt{f}$ and bending back toward the P–K law [19,28]. This empirical relationship was used to design the current pressure drop apparatus and select the operation range such that no degradation occurred prior to the pressure drop measurement section. However, downstream of the measurement section was a needle valve that controlled the flowrate, which produced sufficiently high shear rates to rapidly degrade PEO via chain scission (i.e., breaking of the carbon-carbon and carbon-oxygen bonds that make up the polymer backbone). Thus, mechanically degraded samples were produced by passing a sample through the pressure drop apparatus with the needle valve in a predetermined position prior to passing them through a second time to characterize the degraded samples.

An example of a characterization of a degraded sample from this study is provided in Fig. 4. Here, a sample with an initial molecular weight $M_{wi} = 2 \times 10^6$ g/mol was degraded to $M_{wf} = 0.6 \times 10^6$ g/mol. For comparison, results from a nondegraded $M_w = 2 \times 10^6$ g/mol sample are also provided along with the P–K law (Eq. (1)) and the MDR asymptote (Eq. (2)). The impact of mechanical degradation on the polymer behavior is apparent from the onset of drag reduction for the degraded sample

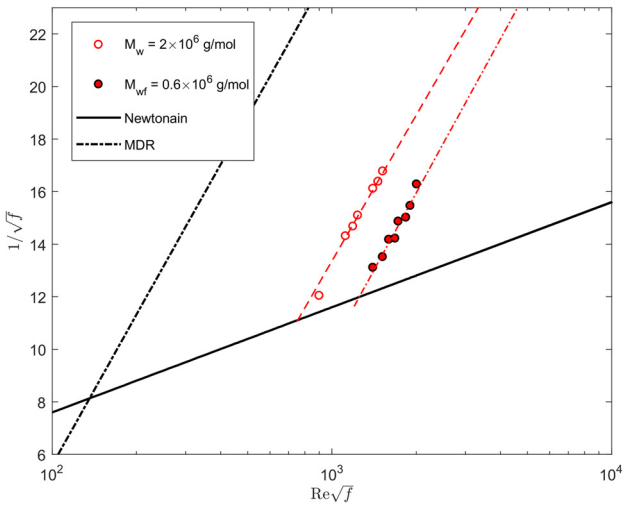

Fig. 4 P–K plot using PEO at an initial $M_{wi} = 2 \times 10^6$ g/mol and $C = 500$ ppm. One of the samples was degraded to a lower molecular weight ($M_w = 0.6 \times 10^6$ g/mol) while the other was nondegraded.

shifted to the right (i.e., to high Reynolds numbers and shear rates) compared to the nondegraded sample. This is consistent with Vanapalli et al. [30,41] that the lower the mean molecular weight the higher the shear rate at the onset of drag reduction. A summary of the degraded results that had a corresponding nondegraded sample are given in Table 3, which includes the nominal initial molecular weight (M_{wi}) and final molecular weight (M_{wf}) as well as the polymeric regime characterization parameters.

4 Discussion and Analysis

4.1 Drag Reduction Performance. Polymer drag reduction generally is defined based on the reduction of the wall shear stress relative to the Newtonian (e.g., water) flow. For pipe flows, the drag reduction efficiency of a polymer solution can be quantified based on the change in the slope relative to the P–K law (i.e., the slope increment, δ). Thus, to quantify the impact of mechanical degradation on the drag reduction ability of the polymer, degraded and nondegraded samples with the same onset of drag reduction (i.e., nominal mean molecular weight) and concentration were characterized and their resulting slope increments compared. These pairs of degraded/nondegraded samples with matching mean molecular weights were identified as described in Sec. 2.1 and listed in Table 3. As an example, three of these degraded/nondegraded pairs are plotted using P–K coordinates in Fig. 5. These pairs were selected to show that concentration only weakly impacted the deviations of the slope increments; there are some conditions where the matched pairs have negligible variation and other conditions that produced significant variation. Prior to

Downloaded from http://asmedigitalcollection.asme.org/fluidsengineering/article-pdf/142/9/091201/6537180/fe_142_09_091201.pdf by guest on 05 December 2021

Table 3 Summary of degraded PEO samples tested in the pressure drop apparatus

$M_{wi} \times 10^{-6}$ (g/mol)	$M_{wf} \times 10^{-6}$ (g/mol)	C (wppm)	Re $\times 10^{-3}$ at C_{max} range	δ	γ^* (1/s)	$\gamma \times 10^{-3}$ range (1/s)
5.0	1.0	500	15–25	22.5	2800	4.2–8.1
4.0	1.0	500	15–30	20.6	3000	4.5–12
4.0	2.0	50–500	12–28	4.5–11.0	1600	1.8–10
5.0	2.0	500	12–24	16.6	2000	3.3–7.6
5.0	4.0	5	8–24	6.1	900	1.2–8.8
2.0	0.6	200–500	18–31	3.5–10.1	6090	7.7–15
1.0	0.6	500	16–27	2.8	7200	1.7–4.9

Molecular weights listed are based on the nominal manufacturer specifications, see Table 2 for corresponding measurements.

exploring the cause for these observations, the specifics of these representative conditions are discussed.

First, examination of the two pairs in Fig. 5 that had $M_{wi} = 4 \times 10^6$ g/mol degraded to $M_{wf} = 2 \times 10^6$ g/mol with either $C = 100$ ppm or 500 ppm shows excellent agreement between the degraded and nondegraded samples for both pairs. The maximum relative difference between degraded and nondegraded samples was ~5%, which is within measurement uncertainty. However, the deviation appears to increase slightly with increasing concentration, which suggests that the slope increment deviation could have a potential weak concentration dependence. While these first two pairs indicated that mechanical degradation had a negligible impact on the drag reduction performance if the mean molecular weight was matched, the other degraded/nondegraded pair ($M_{wi} = 2 \times 10^6$ g/mol degraded to $M_{wf} = 0.6 \times 10^6$ g/mol with $C = 500$ ppm) in Fig. 5 reveals a significant difference in slope increment. Since the concentration was matched with one of the $M_{wi} = 4 \times 10^6$ g/mol samples, the deviation must be dependent on the initial and/or final molecular weights of the polymer solution. Also note that all of the degraded samples have a larger slope increment (i.e., more efficient at reducing drag) relative to their nondegraded samples, even for the first two pairs that had minimal deviation.

Based on observations from previous work [38], the similarity between the first two degraded/nondegraded pairs indicate that within the range of Reynolds numbers tested (Re < 35,000), the longer chains were not preferentially extended over other comparable but slightly shorter chains. Thus, the difference in chain size must not have been sufficient to drastically change the flow characteristics of the solution, and therefore, no significant difference in bulk behavior was observed. However, for the other degraded/nondegraded pair, the significantly improved drag reduction performance with degraded polymer suggests that there are longer chains in the degraded sample because the magnitude of drag reduction rather strongly depends on the longest polymer chains in the solution. Gampert and Wagner [38] showed that a Reynolds number of 20,000 was enough to degrade the fractions of large chains. Since the Reynolds number range of this study exceeds 20,000, these observations indicate preferential stretching and degradation that suggests that deviations are associated with changes in the molecular weight distribution. This is further examined subsequently.

The slope increment is sensitive to the polymer concentration, polymer-solvent combination, and molecular weight [61]. This complicates the comparison between individual degraded/nondegraded pairs because the molecular weight sets the range of polymer concentrations that can be tested in a given pressure drop apparatus (i.e., higher molecular weight samples require lower concentrations than lower molecular weight samples). That prevents the possibility of fixing all of the conditions at a single concentration and polymer-solvent combination to study the dependence of the slope deviation on molecular weight. However, Virk [61] compared numerous combinations of polymer types and solvents and showed that the slope increment is well approximated as being proportional to the square root of concentration. The slope increments from the current results for degraded/nondegraded 0.6 and 2.0×10^6 g/mol samples are plotted versus concentrations (C) in Fig. 6. The results are well approximated by best fit curves having slopes of 0.5, which the power-law fit to the raw data produces exponents that were ±5% of 0.5 for all conditions. These results capture the sensitivity of

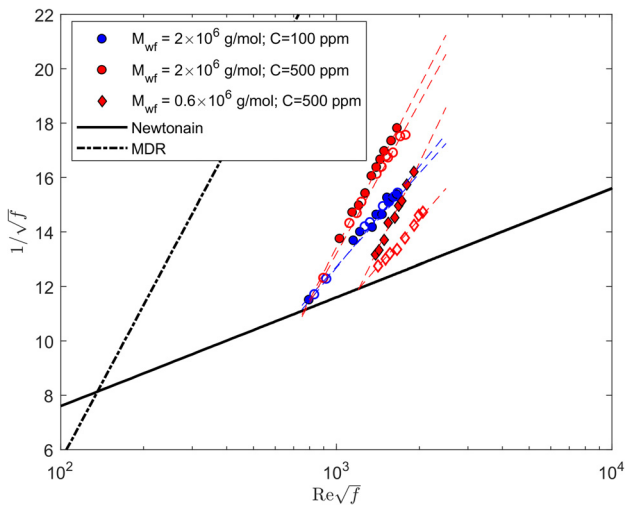

Fig. 5 P–K plot comparing degraded and nondegraded samples with $M_{wf} = 2 \times 10^6$ g/mol (degraded samples had $M_{wi} = 4 \times 10^6$ g/mol) or 0.6×10^6 g/mol (degraded sample had $M_{wi} = 2 \times 10^6$ g/mol). Filled markers represent degraded samples.

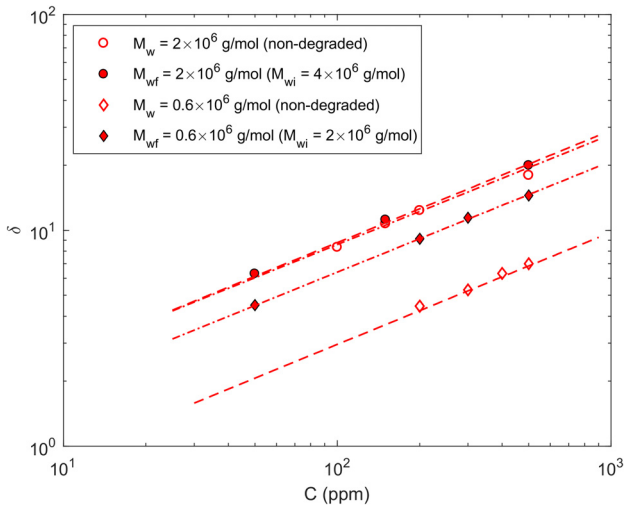

Fig. 6 Slope increment versus concentration (C) for degraded and nondegraded samples of $M_w = 0.6 \times 10^6$ or 2.0×10^6 g/mol. The dashed lines are all best fit curves with a slope of ~0.5.

Downloaded from http://asmedigitalcollection.asme.org/fluidsengineering/article-pdf/142/9/091201/6537180/fe_142_09_091201.pdf by guest on 05 December 2021

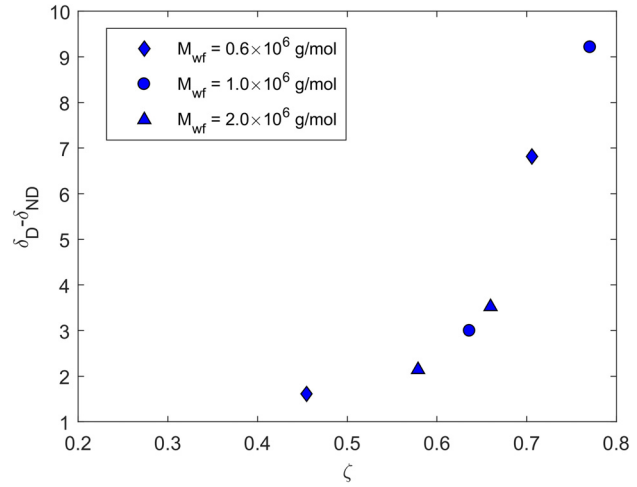

Fig. 7 The difference between the degraded and nondegraded slope increments for $C = 500$ ppm plotted versus the normalized difference between the initial and final molecular weights, $\zeta = (M_{wi} - M_{wf})/M_{wi}$

the slope increment to molecular weight as well as the discrepancy observed in Fig. 5 between the degraded and nondegraded $M_w = 0.6 \times 10^6$. It also shows that the slope increment for the degraded samples maintain the same $C^{1/2}$ dependence as nondegraded samples, which again indicates that the deviations with degradation must be related to molecular weight distribution.

The discussion of Fig. 5 noted that the deviation between the slope increment of degraded (δ_D) and nondegraded (δ_{ND}) samples must be dependent on the initial and/or final molecular weights of the samples. Since the slope increment deviation ($\delta_D - \delta_{ND}$) should approach zero as degradation approaches zero, a reasonable parameter to scale the deviation is the difference between the initial and final molecular weights. This difference was normalized with initial molecular weight to make the scaling parameter, $\zeta = (M_{wi} - M_{wf})/M_{wi}$. Figure 7 plots the slope increment deviation ($\delta_D - \delta_{ND}$) as a function of ζ for $C = 500$ ppm. The first observation from these results is that for all conditions the degraded slope increment was higher than the corresponding nondegraded slope increment (i.e., the slope increment deviation is never negative). In addition, these results show a relatively small deviation for $\zeta < 0.6$, followed by a rapid increase in the deviation. Note that the slope increments for these conditions ranged from 6 to 22.

4.2 Polydispersity. Since testing was performed within the same flow operation range (Reynolds number, geometry, etc.), the deviation must be the product of variations within polymer properties. Most PEO polymer properties (e.g., relaxation time, viscosity ratio, length ratio) are primarily a function of the molecular weight and concentration. Since the concentration and mean molecular weight (i.e., onset of drag reduction shear rate) are equal between the degraded and nondegraded PEO samples, the deviation in performance within the polymeric regime must be related to variations in the distribution of the molecular weight. This assessment is supported by Paterson and Abernathy [31] that determined that the postdegradation molecular weight distribution (e.g., polydispersity) is critical to interpreting polymer flow properties. Furthermore, Hunston and Zakin [37] studied the effect of mechanical degradation (flow-assisted degradation) on the molecular weight distribution of polystyrene. Turbulent measurements, like those in this study, were used to broaden the range of conditions that could be studied with viscosity or GPC methods. Hunston and Zakin [37] showed that for polystyrene the onset of drag reduction was dependent on the molecular weight with the results biased toward the largest molecules in the sample, and that flowrate dependence was related to the shape of the top part of the molecular weight distribution. This supports the assessment that the deviations in slope increment with the PEO samples were likely the product of a change in the molecular distribution (polydispersity) of the samples.

While this suggests that the deviations are related to changes in the molecular weight distribution, it does not explain the consistent improvement of the degraded samples relative to the nondegraded (at the same mean molecular weight) samples. The longer chain molecules have the greatest impact on determining the flow properties of a solution due to their preferential mode of extension [38], which suggests that the current samples (especially those with the largest ζ) had a larger percentage of the longer chain molecules than the nondegraded samples. In general, mechanical degradation narrows the molecular weight distribution if the shear rate is relatively uniformly applied [32,50]. Wall-bounded flows (e.g., pipes, boundary layers) do not have uniformly applied shear rates, which results in a relatively small percentage of the chains being stretched to lengths comparable to the polymer contour length (i.e., maximum polymer extension length) at any instance in time [62,63]. However, if the polymer chains are exposed to the turbulent wall-bounded flow for a sufficiently long period of time, a steady-state condition can be achieved once a sufficient number of stretching/degradation cycles are achieved [11]. If the elongational rate far exceeds that of the critical elongational rate, then the midpoint scission assumption [33–35] would be violated and the final (steady-state) distribution would be broader than the initial [36]. Prior to achieving steady-state conditions, the molecular weight distribution would be asymmetric and biased toward higher molecular weights because at each time-step some percentage of chains would not have broken yet. This suggests that the current results correspond to an intermediate stage of degradation (i.e., prior to achieving steady-state behavior), which was confirmed by comparing the results after multiple passes through the pressure drop apparatus.

The deviation in slope increment for $\zeta > 0.6$ is also indicative of the fact that a mere presence of a few long-chain polymer molecules within a solution can be responsible for significantly increasing the drag reduction. That is to, say, these small fractions of long-chain molecules have a greater impact in defining the flow properties of a degraded sample, than the mean molecular weight of the sample [31]. The validity of this claim within the specified regime of ζ is also subject to the Reynolds number range tested, which for this study was rarely above 30,000. For this range of Reynolds numbers, it could be justified to say that the long chain polymers show preferential extension over the shorter chains and therefore control flow properties of the solutions. Such a behavior is expected to be more pronounced when the disparity between short chains and long chains within a solution is large (disparity in terms of their molecular weight averages). Although Gampert and Wagner [38] used artificially created polydispersed synthesized PAM solutions, they reached the same conclusions, which provides additional support to the validity of these conclusions.

The functional relationship for the ζ dependence as shown in Fig. 7, and more specifically the value where significant variation was observed, is most likely specific to the degradation process. If the residence time were increased, it is presumed that a larger value of ζ could be achieved without significant deviations in the slope increment since any variation would be the product of the broadening of the distribution [36] rather than an excess of larger molecules. As the ratio of the residence time to relaxation time becomes large, the steady-state molecular weight would be achieved and the impact of ζ is expected to significantly decrease if these assumptions are valid. This was tested by creating a PEO polymer ocean with $C = 100$ ppm within the Oklahoma State University 6-in. low-turbulence, recirculating water tunnel [65]. This allowed the facility to be operated for as long as was required to achieve a steady-state mean molecular weight (based on the onset of drag reduction). In addition, the speeds were selected so that the steady-state molecular weights matched two of the

Downloaded from http://asmedigitalcollection.asme.org/fluidsengineering/article-pdf/142/9/091201/6537180/fe_142_09_091201.pdf by guest on 05 December 2021

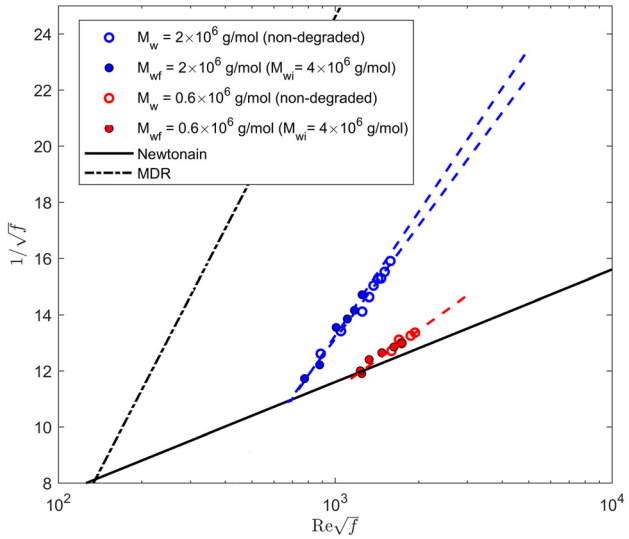

Fig. 8 P–K plot comparing a steady-state degraded sample from a $C = 100$ ppm PEO polymer ocean in a recirculating water tunnel with that of a nondegraded sample

nondegraded molecular weights (M_{wf} of 0.6×10^6 g/mol and 2×10^6 g/mol). The results for the steady-state degraded samples are shown in Fig. 8 along with their corresponding nondegraded samples. The deviations in the slope increment for the 0.6×10^6 g/mol and 2×10^6 g/mol samples were $\delta_D - \delta_{\mathrm{ND}} < 0.5\,(\zeta = 0.8)$ and $\delta_D - \delta_{\mathrm{ND}} = 1.3$ ($\zeta = 0.5$), respectively. These variations are within the measurement uncertainty and illustrate the difference from that observed in Fig. 7, which supports the conjecture that these deviations can be mitigated if steady-state conditions can be achieved.

5 Conclusion

This study uses a turbulent pipe flow experiment to do a comparative analysis between mechanically degraded polymer (PEO) solutions and nondegraded polymer (PEO) solutions at the same mean molecular weight. Degraded samples were produced via passing samples through a pipe that included a precisely positioned V-shaped needle valve. The degradation resulted in an increase in the shear rates at the onset of drag reduction, which Vanapalli et al. [30] provided an empirical relationship between the onset of drag reduction shear rate and the mean molecular weight for PEO. The samples were degraded such that they produced mean molecular weights (onset of drag reduction shear rates) that matched available nondegraded molecular weights. Characterization of the nondegraded samples produced bulk flow behavior that is consistent with previous PEO studies in the literature [28,30,38,61].

Comparative analysis of the mechanically degraded samples (samples with different initial, but known, mean molecular weights degraded to a specific final mean molecular weight) with the nondegraded samples at the mean molecular weight of the final state of the degraded samples showed that while some conditions showed good agreement in the slope increment between the degraded and nondegraded samples (Fig. 5), there were conditions that had significant deviations in the slope increment (drag reduction performance). The nondegraded samples consistently produced larger (more efficient) slope increments. The deviation in slope increment scaled well with the normalized difference between the initial and final molecular weights, $\zeta = (M_{wi} - M_{wf})/M_{wi}$, with the deviation increasing rapidly when $\zeta > 0.6$. However, it is expected that the exact value of this acceleration is specific to the degradation method, including the ratio of the residence time to the relaxation time. The deviations in drag reduction performance between the degraded and nondegraded samples (at the same molecular weight) were attributed to deviations in the molecular weight distribution, which was supported by other observations in the literature [31,37]. Furthermore, this behavior is likely enhanced prior to achieving steady-state molecular weight when there would be an excess of longer polymer chains [38], which was the case for the majority of conditions presented. Finally, it was shown that the amount of deviation can be reduced if steady-state conditions can be achieved. However, if the elongational rate far exceeds the critical elongational rate, then the final molecular weight distribution could be broader [36], which could still impact the drag reduction performance.

These results provide criteria that should be followed if comparisons in drag reduction performance will be made between mechanically (flow-assisted) degraded and nondegraded samples. These results are particularly valuable when using high molecular weight PEO samples at relatively low concentrations (i.e., common drag reduction operation conditions) since the common viscosity and GPC approaches are not well suited for these conditions [38,59]. This also enables a robust means of establishing polymeric oceans that can be compared with previous nondegraded samples, which can greatly simplify fundamental PDR studies of developing turbulent boundary layers by removing the concentration dependence.

Acknowledgment

These authors would like to thank Dr. Frank Blum and Dr. Siva Vanapalli for discussions on the use of GPC for analysis of high-molecular weight PEO as well as Marcus Lander, Jacquelyne Baade, and JW Wallace who have assisted with experiments.

Funding Data

- National Science Foundation (Grant No. 1604978; Funder ID: 10.13039/100000001).

References

[1] Mysels, K. J., 1947, "Flow of Thickened Fluids," U.S. Patent No. 2,492,173.
[2] Toms, B. A., 1949, "Some Observations on the Flow of Linear Polymer Solutions Through Straight Tubes at Large Reynolds Numbers," Proceedings of the First International Congress on Rheology, Vol. 2, North-Holland, Amsterdam, Sept. 21–24, 1948, pp. 135–141.
[3] Toms, B. A., 1949, "Detection of a Wall Effect in Laminar Flow of Solutions of a Linear Polymer," J. Colloid Sci., **4**(5), pp. 511–521.
[4] Hoyt, J. W., 1972, "The Effect of Additives on Fluid Friction," ASME J. Fluids Eng., **94**(2), pp. 258–285.
[5] Burger, E. D., Chorn, L. G., and Perkins, T. K., 1980, "Studies of Drag Reduction Conducted Over a Broad Range of Pipeline Conditions When Flowing Prudhoe Bay Crude Oil," J. Rheol., **24**(5), pp. 603–626.
[6] Sellin, R., Hoyt, J., Poliert, J., and Scrivener, O., 1982, "The Effect of Drag Reducing Additives on Fluid Flows and Their Industrial Applications: Part 2—Present Applications and Future Proposals," J. Hydraulic Res., **20**(3), pp. 235–292.
[7] Fruman, D. H., and Aflalo, S. S., 1989, "Tip Vortex Cavitation Inhibition by Drag-Reducing Polymer Solutions," ASME J. Fluids Eng., **111**(2), pp. 211–216.
[8] White, C. M., and Mungal, M. G., 2008, "Mechanics and Prediction of Turbulent Drag Reduction With Polymer Additives," Annu. Rev. Fluid Mech., **40**(1), pp. 235–256.
[9] Elbing, B. R., Dowling, D. R., Perlin, M., and Ceccio, S. L., 2010, "Diffusion of Drag-Reducing Polymer Solutions Within a Rough-Walled Turbulent Boundary Layer," Phys. Fluids, **22**(4), p. 045102.
[10] Elbing, B. R., Winkel, E. S., Ceccio, S. L., Perlin, M., and Dowling, D. R., 2010, "High-Reynolds-Number Turbulent-Boundary-Layer Wall-Pressure Fluctuations With Dilute Polymer Solutions," Phys. Fluids, **22**(8), p. 085104.
[11] Elbing, B. R., Solomon, M. J., Perlin, M., Dowling, D. R., and Ceccio, S. L., 2011, "Flow-Induced Degradation of Drag-Reducing Polymer Solutions Within a High-Reynolds-Number Turbulent Boundary Layer," J. Fluid Mech., **670**, pp. 337–364.
[12] Elbing, B. R., Perlin, M., Dowling, D. R., and Ceccio, S. L., 2013, "Modification of the Mean Near-Wall Velocity Profile of a High-Reynolds Number Turbulent Boundary Layer With the Injection of Drag-Reducing Polymer Solutions," Phys. Fluids, **25**(8), p. 085103.

Downloaded from http://asmedigitalcollection.asme.org/fluidsengineering/article-pdf/142/9/091201/6537180/fe_142_09_091201.pdf by guest on 05 December 2021

[13] Perlin, M., Dowling, D. R., and Ceccio, S. L., 2016, "Freeman Scholar Review: Passive and Active Skin-Friction Drag Reduction in Turbulent Boundary Layers," ASME J. Fluids Eng., **138**(9), p. 091104.
[14] Elbing, B. R., 2018, "Flow-Assisted Polymer Degradation in Turbulent Boundary Layers," Proceedings of the AIChE Annual Meeting, Area 01C Interfacial Phenomena 590e, Pittsburgh, PA, Oct. 28–Nov. 2, 2018, pp. 1–8.
[15] McGary, C. W., Jr., 1960, "Degradation of Poly(Ethylene Oxide)," J. Polym. Sci., **46**(147), pp. 51–57.
[16] Shin, H., 1965, "Reduction of Drag in Turbulence by Dilute Polymer Solutions," Ph.D. dissertation, Massachusetts Institute of Technology, Cambridge, MA.
[17] Bailey, F. E., Jr., and Koleske, J. V., 1976, *Poly(Ethylene Oxide)*, Academic Press, New York.
[18] Bortel, E., and Lamot, R., 1977, "Examination of the Breakdown of High Molecular Weight Polyethylene Oxides in the Solid State," Macromol. Chem. Phys., **178**(9), pp. 2617–2628.
[19] Moussa, T., and Tiu, C., 1994, "Factors Affecting Polymer Degradation in Turbulent Pipe Flow," Chem. Eng. Sci., **49**(10), pp. 1681–1692.
[20] Fore, R. S., Szwalek, J., and Sirviente, A., 2005, "The Effects of Polymer Solution Preparation and Injection on Drag Reduction," ASME J. Fluids Eng., **127**(3), pp. 536–549.
[21] Layec-Raphalen, M. N., and Layec, Y., 1985, "Influence of Molecular Parameters on Laminar Non-Newtonian and on Turbulent Flows of Dilute Polymer Solutions," *The Influence of Polymer Additives on Velocity and Temperature Fields, International Union of Theoretical and Applied Mechanics* (Deutsche Rheologische Gasellschaft), B. Gampert, ed., Springer, Berlin, Heidelberg, pp. 89–100.
[22] Yarin, A. L., 1991, "Strong Flows of Polymeric Liquids: Part 2. Mechanical Degradation of Macromolecules," J. Non-Newtonian Fluid Mech., **38**(2–3), pp. 127–136.
[23] Yarin, A. L., 1993, *Free Liquid Jets and Films: Hydrodynamics and Rheology*, Longman Publishing Group, New York.
[24] Yarin, A. L., 1997, "On the Mechanism of Turbulent Drag Reduction in Dilute Polymer Solutions: Dynamics of Vortex Filaments," J. Non-Newtonian Fluid Mech., **69**(2–3), pp. 137–153.
[25] Zaitoun, A., Makakou, P., Blin, N., Al-Maamari, R. S., Al-Hashmi, A.-A. R., and Abdel-Goad, M., 2012, "Shear Stability of EOR Polymers," SPE J., **17**(02), pp. 335–339.
[26] Fontaine, A., Petrie, H., and Brungart, T., 1992, "Velocity Profile Statistics in a Turbulent Boundary Layer With Slot-Injected Polymer," J. Fluid Mech., **238**, pp. 435–466.
[27] Petrie, H., Fontaine, A., Money, M., and Deutsch, S., 2005, "Experimental Study of Slot-Injected Polymer Drag Reduction," Proceedings of the Second International Symposium on Seawater Drag Reduction, Busan, Korea, May 23–26, pp. 605–620.
[28] Elbing, B. R., Winkel, E. S., Solomon, M. J., and Ceccio, S. L., 2009, "Degradation of Homogeneous Polymer Solutions in High Shear Turbulent Pipe Flow," Exp. Fluids, **47**(6), pp. 1033–1044.
[29] Culter, J. D., Zakin, J. L., and Patterson, G. K., 1975, "Mechanical Degradation of Dilute Solutions of High Polymers in Capillary Tube Flow," J. Appl. Polym. Sci., **19**(12), pp. 3235–3240.
[30] Vanapalli, S. A., Islam, M. T., and Solomon, M. J., 2005, "Scission-Induced Bounds on Maximum Polymer Drag Reduction in Turbulent Flow," Phys. Fluids, **17**(9), p. 095108.
[31] Paterson, R. W., and Abernathy, F. H., 1970, "Turbulent Flow Drag Reduction and Degradation With Dilute Polymer Solutions," J. Fluid Mech., **43**(4), pp. 689–710.
[32] Yu, J. F. S., Zakin, J. L., and Patterson, G. K., 1979, "Mechanical Degradation of High Molecular Weight Polymers in Dilute Solution," J. Appl. Polym. Sci., **23**(8), pp. 2493–2512.
[33] Hinch, E. J., 1977, "Mechanical Models of Dilute Polymer Solutions in Strong Flows," Phys. Fluids, **20**(10), pp. S22–S30.
[34] Horn, A., and Merrill, E., 1984, "Midpoint Scission of Macromolecules in Dilute Solution in Turbulent Flow," Nature, **312**(5990), pp. 140–141.
[35] Odell, J. A., Keller, A., and Miles, M. J., 1983, "Method for Studying Flow-Induced Polymer Degradation: Verification of Chain Halving," Polym. Commun., **24**(1), pp. 7–10.
[36] Sim, H., Khomami, B., and Sureshkumar, R., 2007, "Flow–Induced Chain Scission in Dilute Polymer Solutions: Algorithm Development and Results for Scission Dynamics in Elongational Flow," J. Rheol., **51**(6), pp. 1223–1251.
[37] Hunston, D. L., and Zakin, J. L., 1980, "Flow-Assisted Degradation in Dilute Polystyrene Solutions," Polym. Eng. Sci., **20**(7), pp. 517–523.
[38] Gampert, B., and Wagner, P., 1985, "The Influence of Molecular Weight and Molecular Weight Distribution on Drag Reduction and Mechanical Degradation in Turbulent Flows of Highly Dilute Polymer Solutions," *The Influence of Polymer Additives on Velocity and Temperature Fields, International Union of Theoretical and Applied Mechanics* (Deutsche Rheologische Gasellschaft), B. Gampert, ed., Springer, Berlin, Heidelberg, pp. 71–85.
[39] Habibpour, M., and Clark, P. E., 2017, "Drag Reduction Behavior of Hydrolyzed Polyacrylamide/Xanthan Gum Mixed Polymer Solutions," Pet. Sci., **14**(2), pp. 412–423.
[40] Lumley, J. L., 1973, "Drag Reduction in Turbulent Flow by Polymer Additives," J. Polym. Sci., **7**(1), pp. 263–290.
[41] Vanapalli, S. A., Ceccio, S. L., and Solomon, M. J., 2006, "Universal Scaling for Polymer Chain Scission in Turbulence," Proc. Natl. Acad. Sci., **103**(45), pp. 16660–16665.
[42] Grandbois, M., Beyer, M., Rief, M., Clausen-Schaumann, H., and Gaub, H. E., 1999, "How Strong is a Covalent Bond?," Science, **283**(5408), pp. 1727–1730.
[43] White, C. M., Somandepalli, V. S. R., and Mungal, M. G., 2004, "The Turbulence Structure of Drag-Reduced Boundary Layer Flow," Exp. Fluids, **36**(1), pp. 62–69.
[44] Hou, Y. X., Somandepalli, V. S. R., and Mungal, M. G., 2008, "Streamwise Development of Turbulent Boundary-Layer Drag Reduction With Polymer Injection," J. Fluid Mech., **597**, pp. 31–66.
[45] Somandepalli, V. S. R., Hou, Y. X., and Mungal, M. G., 2010, "Concentration Flux Measurements in a Polymer Drag-Reduced Turbulent Boundary Layer," J. Fluid Mech., **644**, pp. 281–319.
[46] White, C. M., Dubief, Y., and Klewicki, J., 2012, "Re-Examining the Logarithmic Dependence of the Mean Velocity Distribution in Polymer Drag Reduced Wall-Bounded Flow," Phys. Fluids, **24**(2), p. 021701.
[47] Escudier, M., Rosa, S., and Poole, R., 2009, "Asymmetry in Transitional Pipe Flow of Drag-Reducing Polymer Solutions," J. Non-Newtonian Fluid Mech., **161**(1–3), pp. 19–29.
[48] Farsiani, Y., Saeed, Z., and Elbing, B. R., 2019, "Modification of Turbulent Boundary Layer in the Homogeneous Polymeric Drag Reduced Flow," APS Division of Fluid Dynamics Annual Meeting, Bulletin of the American Physical Society, 64(13), Seattle, WA, Nov. 23–26, Paper No. M01.
[49] Farsiani, Y., Saeed, Z., Jayaraman, B., and Elbing, B. R., 2020, "Modification of Turbulent Boundary Layer Coherent Structures With Drag Reducing Polymer Solution," Phys. Fluids, **32**(1), p. 015107.
[50] Kim, C. A., Kim, J. T., Lee, K., Choi, H. J., and Jhon, M. S., 2000, "Mechanical Degradation of Dilute Polymer Solutions Under Turbulent Flow," Polymers, **41**(21), pp. 7611–7615.
[51] Kalashnikov, V. N., 2002, "Degradation Accompanying Turbulent Drag Reduction by Polymer Additives," J. Non-Newtonian Fluid Mech., **103**(2–3), pp. 105–121.
[52] Draad, A. A., Kuiken, G., and Nieuwstadt, F., 1998, "Laminar–Turbulent Transition in Pipe Flow for Newtonian and Non-Newtonian Fluids," J. Fluid Mech., **377**, pp. 267–312.
[53] Petrie, H. L., Deutsch, S., Brungart, T. A., and Fontaine, A. A., 2003, "Polymer Drag Reduction With Surface Roughness in Flat-Plate Turbulent Boundary Layer Flow," Exp. Fluids, **35**(1), pp. 8–23.
[54] De Gennes, P.-G., 1979, *Scaling Concepts in Polymer Physics*, Cornell University Press, Ithaca, NY.
[55] Bailey, F. E., Jr., and Callard, R. W., 1959, "Some Properties of Poly(Ethylene Oxide) in Aqueous Solution," J. Appl. Polym. Sci., **1**(1), pp. 56–62.
[56] Lander, M., 2018, "Preparation and Characterization of Polyethylene-Oxide (PEO) Solution," M.S. thesis, Oklahoma State University, Stillwater, OK.
[57] McKeon, B. J., 2007, "Measurement of Pressure With Wall Tappings," *Handbook of Experimental Fluid Mechanics*, C. Tropea, A. L. Yarin, and J. F. Foss, eds., Springer, Heidelberg, Germany, pp. 180–184.
[58] Kulik, V. M., 2001, "Drag Reduction Change of Polyethyleneoxide Solutions in Pipe Flow," Exp. Fluids, **31**(5), pp. 558–566.
[59] Berman, N. S., 1977, "Drag Reduction of the Highest Molecular Weight Fractions of Polyethylene Oxide," Phys. Fluids, **20**(5), pp. 715–718.
[60] Virk, P. S., Merrill, E. W., Mickle, H. S., Smith, K. A., and Mollo-Christensen, E. L., 1967, "The Toms Phenomenon: Turbulent Pipe Flow of Dilute Polymer Solutions," J. Fluid Mech., **30**(2), pp. 305–328.
[61] Virk, P. S., 1975, "Drag Reduction Fundamentals," AIChE J., **21**(4), pp. 625–656.
[62] Dubief, Y., White, C. M., Terrapon, V. E., Shaqfeh, E. S., Moin, P., and Lele, S. K., 2004, "On the Coherent Drag-Reducing and Turbulence-Enhancing Behavior of Polymers in Wall Flows," J. Fluid Mech., **514**, pp. 271–280.
[63] Gupta, V., Sureshkumar, R., and Khomami, B., 2004, "Polymer Chain Dynamics in Newtonian and Viscoelastic Turbulent Channel Flows," Phys. Fluids, **16**(5), pp. 1546–1566.
[64] Winkel, E. S., Oweis, G. F., Vanapalli, S. A., Dowling, D. R., Perlin, M., Solomon, M. J., and Ceccio, S. L., 2009, "High-Reynolds-Number Turbulent Boundary Layer Friction Drag Reduction From Wall-Injected Polymer Solutions," J. Fluid Mech., **621**, pp. 259–288.
[65] Elbing, B. R., Daniel, L., Farsiani, Y., and Petrin, C. E., 2018, "Design and Validation of a Recirculating, High-Reynolds Number Water Tunnel," ASME J. Fluids Eng., **140**(8), p. 081102.

Downloaded from http://asmedigitalcollection.asme.org/fluidsengineering/article-pdf/142/9/091201/6537180/fe_142_09_091201.pdf by guest on 05 December 2021